Received: 9 January 2020 | Revised: 26 May 2020 | Accepted: 27 May 2020

DOI: 10.1002/eng2.12222

RESEARCH ARTICLE

WILEY

Scanning acoustic microscopy analysis of the mechanical properties of polymeric components in photovoltaic modules

Laila V. Mesquita | Djamel Eddine Mansour | Paul Gebhardt | Luciana Pitta Bauermann

Fraunhofer Institute for Solar Energy Systems ISE, Freiburg im Breisgau, Germany

Correspondence
Luciana Pitta Bauermann, Fraunhofer Institute for Solar Energy Systems ISE, Heidenhofstrasse 2, 79110 Freiburg im Breisgau, Germany.
Email: luciana.pitta.bauermann@ise.fraunhofer.de

Abstract

The characterization of mechanical properties of polymeric backsheet and encapsulation foils of photovoltaic (PV) modules usually involves destructive techniques, such as dynamic mechanical analysis and tensile testing. In this article, we validate the scanning acoustic microscopy (SAM) as a nondestructive characterization method to estimate the mechanical properties of polymeric multi-layers in PV modules. The acoustic speed inside each individual material is measured and its mechanical properties calculated. For this validation, other techniques are employed to determine the values of density, thickness, and elastic modulus of the foils. The viscoelastic properties of the polymeric foils are temperature dependent. The longitudinal modulus measured acoustically at 15 MHz and the Young's modulus from conventional tensile testing were compared at different temperatures. Both techniques show good agreement regarding the change in mechanical properties caused by temperature variation. The disagreement in the absolute values of these parameters is explained by the different frequency magnitudes at which both measurements are performed. This confirms that SAM is a reliable technique to measure changes in the viscoelastic properties of the foils in PV modules nondestructively, and thus to obtain more information about aging-induced material changes and degradation.

KEYWORDS

elastic constant, nondestructive analysis, polymeric materials, PV module, scanning acoustic microscopy

1 | INTRODUCTION

Polymeric backsheet (BS) and encapsulation foils are major components of photovoltaic (PV) modules, and along with other critical functions they fulfill, they must provide mechanical stability and module protection against multiple environmental stresses.[1] Since several module failures and defects occur due to polymer degradation and aging during

weathering,[2] understanding changes in the viscoelastic properties of these polymeric foils is of utmost interest to improve their mechanical stability during a module's lifetime and to assess the long-term performance of PV modules. Some of these defects, such as loss in adhesion and delamination, permeation variation, cracks, embrittlement, among others, relate to or are the direct result of changes in the mechanical properties of the polymeric layers.[2-5]

While nondestructive quality testing of PV modules is necessary to qualify individual components embedded, for example, after manufacturing or upon problems in field performance, the characterization of the properties of BS and encapsulation foils inside a PV module is challenging.[6] On the one hand, the mechanical characterization of these foils commonly rely on destructive techniques, such as tensile tests[3] and dynamic mechanical analysis,[7] which potentially restrict further tests in case intact modules are required. Moreover, attempting to extract and separate the laminated module components before their individual characterization is difficult[2] and would incur severe material damage, which inevitably affects the results. Investigating single, nonlaminated foils is often a cheaper, simpler, and more flexible approach to sample preparation, but it does not address material interactions that occur within the PV modules during their service life.[8] On the other hand, the possibility to characterize components laminated inside PV modules by nondestructive techniques is restricted by the availability of techniques.[6] Therefore, the development of nondestructive analyses methods for the mechanical characterization of polymeric components in PV modules is fundamental. Some of the available nondestructive methods used to investigate the mechanical and viscoelastic properties of PV module polymeric materials include, for example, nanoindentation,[9] and acoustic methods.[10,11]

Acoustic measurements deliver information on the behavior of ultrasound upon propagation through materials. The interaction between sound and matter thus reveals material-specific information, such as speed of sound, acoustic attenuation, elastic modulus, density, and crosslinking degree.[10,12,13] Although acoustic methods have been widely employed to characterize a range of materials, including polymers,[12,14,15] their application, particularly at the ultrasound range, to study the mechanical properties of PV module backsheet and encapsulation materials has not been widely documented. In the field of photovoltaics, acoustic waves particularly at the MHz range have often been applied in the qualitative analysis of PV modules for visualizing and detecting several failures and defects within the internal structure of the modules, such as air gaps, voids within the encapsulant, cell cracks,[2,6,16] and interconnect quality in shingled solar cells.[17] Additionally, acoustic methods have also found applications in the determination of crosslinking degree of the encapsulation foil in PV modules[11,13] and its thickness.[18] Besides, because the acoustic properties of polymers depend on both ultrasound frequency and temperature,[15] a thorough characterization of the temperature-frequency dependence of PV module backsheet and encapsulation foils is needed to determine the measurement error and optimal parameter conditions.

The aim of this article is to show a simple approach to characterize the acoustic properties of polyethylene terephthalate (PET)-based backsheet (here referred to as BS) and fast-cure ethylene-vinyl acetate (EVA) encapsulation foil inside a PV module nondestructively using scanning acoustic microscopy (SAM) in pulse-echo mode. The measurements are done at different temperatures and ultrasound frequencies. As a validation step, the properties of the single foils are also characterized and compared with destructive tensile tests of the single foils. This article introduces a novel application of the SAM to measure the viscoelastic properties of polymeric layers in a PV module.

The basic principle of SAM is illustrated in Figure 1. A sound pulse propagates into the sample through the coupling fluid (water). An echo arises as the acoustic wave strikes the specimen's top surface s_1. Part of the acoustic wave propagates through the material's bulk and a second echo arises once the wavefront reflects from its back surface s_2. The time delay between both top and back surface echoes is called the time-of-flight (TOF):

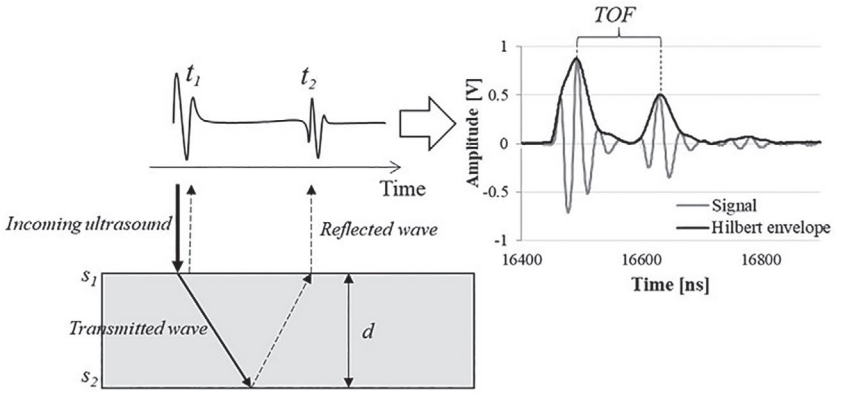

FIGURE 1 Measurement principle of the scanning acoustic microscopy in reflection mode

The speed of sound c can be calculated from the round-trip travel time of the acoustic wave across the thickness of the layer according to the following relation.[15]

$$c = \frac{2\mathrm{d}}{(t_2 - t_1)} \tag{1}$$

with d = thickness and (t_2 - t_1) is the TOF between the echoes from the back s_2 and top surfaces s_1 of the investigated layer. Because a given propagation mode relates to a particular sound speed, the wave mode then determines the corresponding elastic constant, such that as the longitudinal and shear speeds relate to the longitudinal and shear modulus, respectively. In isotropic materials, including polymers, these two propagation modes and the density ρ of a given material can be used to determine the material's elastic constants, particularly the Young's modulus.[10] The mathematical relations are.[10,14,15,19]

$$L = \rho c_l^2, \tag{2}$$

$$G = \rho c_s^2, \tag{3}$$

$$L = K + 4G/3, \tag{4}$$

$$E = 3K(1 - 2\delta) = 2G\,(1 + \delta), \tag{5}$$

where L, G, K, and E are the longitudinal, shear, bulk, and Young's moduli, respectively, and δ = Poisson's ratio. Because in our case the transducer is scanned perpendicularly to the material and liquids or very soft materials do not support shear wave propagation,[7,14] our approach is therefore based on the analysis of longitudinal waves only. Therefore, the experimental results refer to the longitudinal modulus L only.

2 | MATERIAL AND METHODS

2.1 | Samples

Mini-PV modules ($20 \times 20\,\mathrm{cm}^2$) consisting of a commercially available PET-based backsheet (BS), fast-cure EVA encapsulation foil, monocrystalline silicon solar cell, and front solar glass were laminated under standard conditions. Single BS and EVA foils were also laminated at the same conditions as the PV modules. The BS foil consists of a 150 μm PET core layer with outer and inner coating layers (each approximately 10 μm). The thickness of the fast-cure EVA foil before the lamination is around 340 μm thick.

2.2 | Density tests

Pycnometric density measurements (Micro-Ultrapyc 1200e; Quantachrome Instruments, Florida) of the laminated BS and EVA were carried out at 10°C, 15°C, 20°C, 25°C, 30°C, 35°C, and 40°C. Three samples of each polymeric foil were measured and the average values and SDs calculated. These were allowed to reach equilibrium prior to the measurements.

2.3 | Dilatometry

Dilatometry tests (TMA 402 F3 Hyperion; NETZSCH) were employed to investigate thickness changes in the polymeric foils as a function of temperature. Three samples of each foil were let reach equilibrium for at least 24 hours before being measured at 20°C with a dial gauge. Then, the change in thickness of the foils was measured at 10°C, 15°C, 20°C, 25°C, and 30°C (with a load of 0.05 N). The average and SD were calculated.

2.4 | Tensile tests

BS and EVA strips ($10 \times 100\,\mathrm{mm}^2$ and $10 \times 75\,\mathrm{mm}^2$, respectively) were cut out from the laminated rolls. Because of the anisotropy of the BS, measurements of this foil were performed at machine (MD) and transverse direction (TD). Tensile

tests were carried out according to DIN EN ISO 527-3[20] using a Zwick Roell Z010 tensile testing machine coupled to a hot-air oven. The measurements were done at a test speed of 50 mm/min at room temperature (27.3°C), 30°C, 35°C, and 40°C. Five samples of each foil were used for the measurements and the samples were conditioned at the corresponding temperature for 24 hours prior to analysis. The original cross-section of the foil specimens have been previously determined to calculate the tensile stress. The strain was calculated as the ratio of the elongation of the foil (measured from the displacement of the crosshead) to its original gauge length. The initial linear portion of the stress-strain curves was used to calculate the Young's modulus, E. The calculation of the average value with the respective SDs for each temperature and material was done.

2.5 | Acoustic measurements

The laminated samples (single polymeric sheets and PV modules) were placed flat in a water tank and scanned by a scanning acoustic microscope (SAM 500 HD[2], PVA TePla Analytical System GmbH, Westhausen, Germany). The measurements were carried out in pulse-echo mode, at a normal incidence angle at the following acoustic frequencies: 15, 30, and 100 MHz, and at the temperatures of 10°C, 15°C, 20°C, 25°C, 30°C, 35°C, and 40°C. Previous experimental analyses using the frequencies above revealed that they provide good peak resolution for the purposes of this work, that is, the reflection of the acoustic waves at the concerned interfaces yields discernible echoes and the resulting peaks are not overlapping. The samples were allowed to rest for at least 1 hour at the desired temperature to reach equilibrium before each measurement. To keep consistency, the same area was scanned for every temperature and frequency combination and at least five points were collected. The average and the SD are calculated. The received echoes were digitized at a sampling rate of 1.25 GSamples/s. The experimental setup is shown in Figure 1. The reflectograms were interpreted as shown in a previous study.[16] The TOF measurements were calculated based on the peak maxima of the Hilbert transform of the signals.[21] The TOF of the foils were obtained from the SAM and the corresponding longitudinal modulus L was calculated from the measured TOF, density, and thickness. The density and thickness values used were determined from measurements of the single foils (described below). The sound speed c_l in the foils were calculated from Equation (1) $c = 2d/(t_2 - t_1)$ with $(t_2 - t_1)$ being the TOF between the first and back surface echoes of the polymeric foils.

3 | RESULTS AND DISCUSSION

3.1 | Density and thickness

The density of both BS and EVA foils at different temperatures are shown in Figure 2. The experimental results reveal that the density of the BS, although displaying a decreasing trend, does not vary much from 10°C to 30°C, after which a change in behavior takes place, due to the temperature not being held completely stable at the higher temperatures, or possible

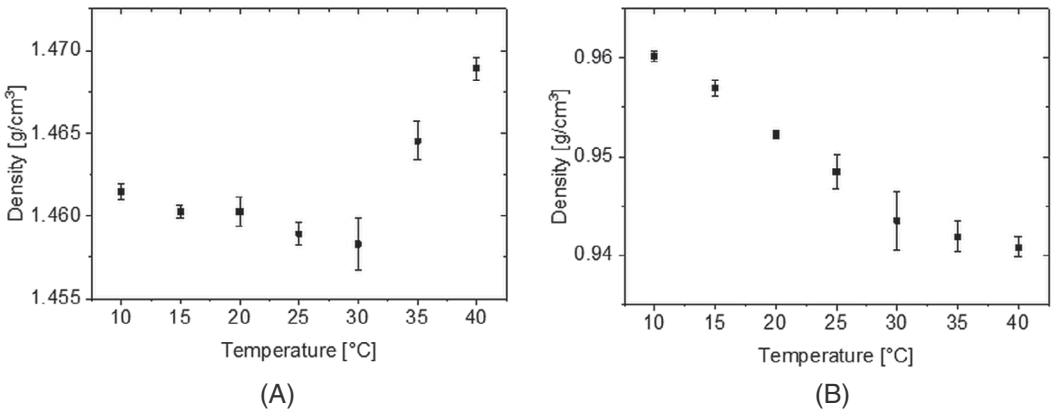

FIGURE 2 Density of the laminated BS, A, and EVA, B, foils as a function of temperature. The points correspond to the average of three measurements and the error bars the respective SDs

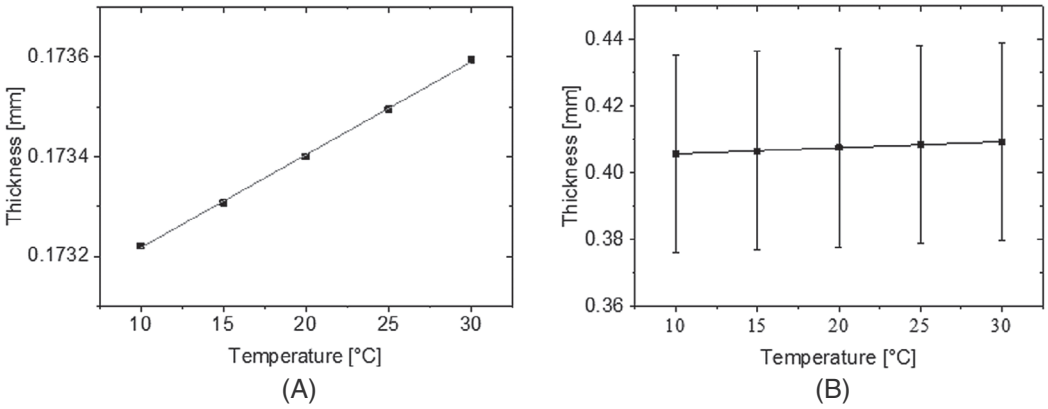

FIGURE 3 Thickness of the laminated BS, A, and EVA, B, foils as a function of temperature. The points correspond to the average of three measurements and the error bars the respective SDs

interactions between the BS samples and the fluid. The density of the fast-cure EVA decreases linearly by 0.07%/°C with increasing temperature.

Figure 3 shows the experimental results from the dilatometry tests. A closer look at the results reveals that the thickness of the polymeric foils increases slightly with increasing temperature. The calculated increase in thickness of BS foil is 0.2% from 10°C to 30°C, whereas the EVA thickness increases by about 0.9%. Moreover, Figure 3B also shows that the variation due to sample heterogeneity in the EVA is much larger (±0.03 mm) than the actual temperature-dependent thickness change. During lamination, the EVA melts and hardens again. This process inevitably led to regions of uneven thickness in the samples. In the dilatometry tests, the same measurement points are used as the samples are gradually heated up before each measurement. Therefore, measurements are taken from samples that present heterogeneous thickness, which ultimately caused the large, but constant thickness deviation at all temperatures, depicted in Figure 3B. Hence, significant variations in the measurements of EVA were expected. However, despite the slight changes in density and thickness, these were assumed negligible in this temperature range. Therefore, these properties were assumed to be constant across the investigated temperature range and average values were used as input to calculate the viscoelastic changes of the foils in the PV modules.

3.2 | Tensile tests

Figure 4 below depicts the Young's modulus (E) of the BS in both orientations MD and TD and fast-cure EVA foils calculated as the slope of the stress-strain curves in the elastic regime. The results show a decrease in E with increasing temperature for both materials.

Figure 4A shows that E-modulus values for the BS in the TD are higher than in the MD at all temperatures measured. Additionally, the behavior of E with temperature in the BS is similar in both foil orientations. The sharpest drop was observed from room temperature (27.3°C) to 30°C in both foil orientations. Then, E decreases more smoothly until to 40°C and reaches a change of 19% in the MD and 14% in the TD, respectively. A strong change in the modulus of the PET-based BS film at this temperature range is not expected since the temperatures investigated lie far below the glass transition temperature, T_g, of PET, that is, 85°C.[1] Nevertheless, room temperature variations during sample measurements might explain the higher deviation observed in the measurements of the foils and thus the sharp modulus drop observed from 27.3°C up to 30°C in the BS. While E varies across different foils, the moduli of several photovoltaic module BS foils containing PET as the core layer have been reported to range from around 2000 to 3100 MPa (at room temperature).[22] By contrast, our experimental results show a considerably higher modulus for the particular foil studied, with values ranging between around 5000 (at room temperature) and 4000 MPa in both MD and TD. Nevertheless, it is also important to mention that the PET-based BS foil used in this study was coated with two thin layers, which have an influence on their elastic behavior, therefore, their E values.

In the EVA foil (Figure 4B) the sharpest drop in E also takes place in the lower temperature range. Then it decreases linearly down to 40°C. This result is expected since we are approaching the melting peak temperature of EVA, T_m, which

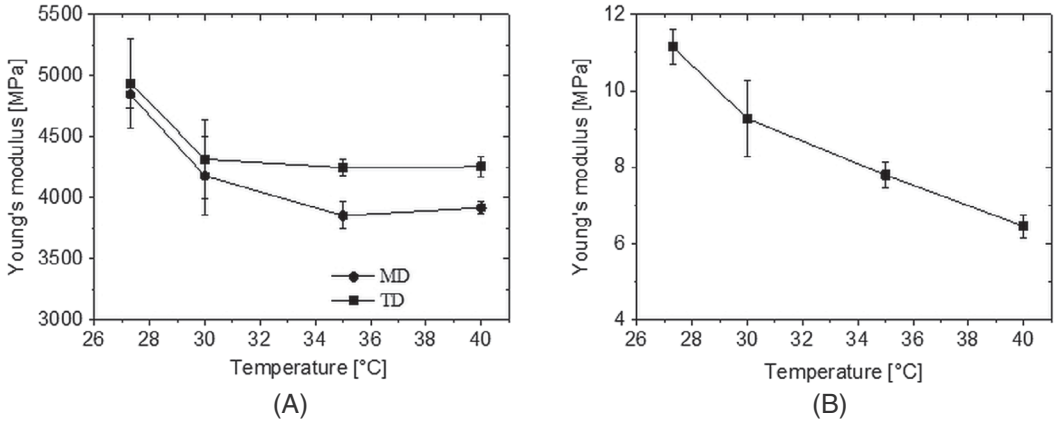

FIGURE 4 Young's modulus (*E*) of BS, A, and EVA, B, at different temperatures, as calculated from the stress–strain curves obtained by tensile tests. The points correspond to the average of five measurements and the error bars the respective SDs

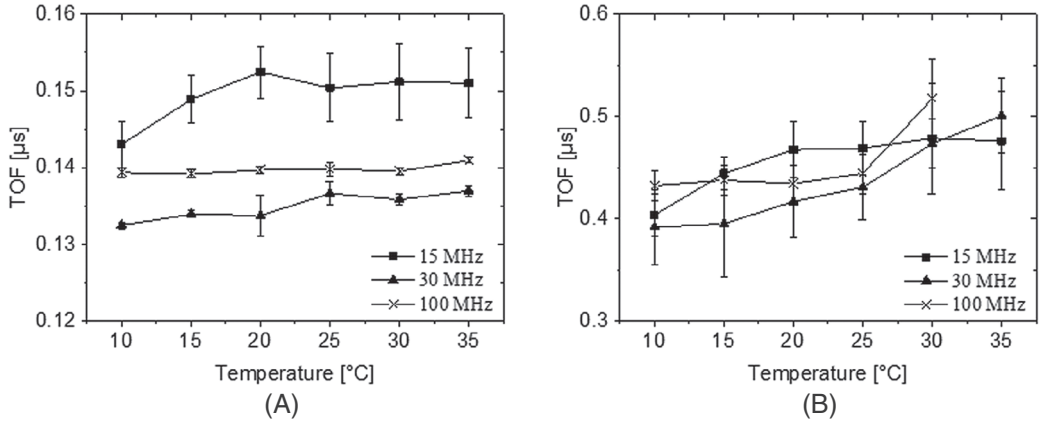

FIGURE 5 Time-of-flight in the individual BS, A, and EVA, B, foils as a function of temperature. The points correspond to the average of five measurements and the error bars show the respective SDs

is around 55°C.[23] The Young's modulus decreases by 42% over the temperature range, reaching a final *E* value of 6.5 MPa. That means that the elasticity in the EVA changes more with temperature compared with the BS. Similar elasticity values for unexposed and aged EVA encapsulant foils have been reported in the literature, where it is shown that the modulus drops considerably after 40°C and tends to reach values below 1 MPa at temperatures higher than $T_{m.}$[2,7] Overall, the results show that the changes in the elastic modulus of the foils are much higher than the changes in density and thickness measured within the temperature range studied.

3.3 | Acoustic properties of freestanding BS and EVA foils

The TOF curves for the freestanding BS and EVA foils as a function of temperature at different frequencies are shown in Figure 5. The data points correspond to the average of five TOF measurements per temperature and frequency. In both polymeric materials, the TOF increases as the temperature rises, with exception of the BS measured at 100 MHz (Figure 5A). In this particularly case, the TOF is constant across the temperature range.

In the BS foil, TOF increases by 6%, 3%, and 1% with increasing temperature at 15, 30, and 100 MHz, respectively. In the EVA foil, larger SDs were observed for all frequencies used (Figure 5B), which might be explained by its large thickness variations. In this case, the TOF increases by 18%, 28%, and 20% with increasing temperature at 15, 30, and 100 MHz, respectively. Therefore, these findings suggest that in terms of TOF, EVA is more sensitive to temperature changes than the BS foil. The same tendency is observed for the Young modulus calculated from the tensile tests. The TOF values were

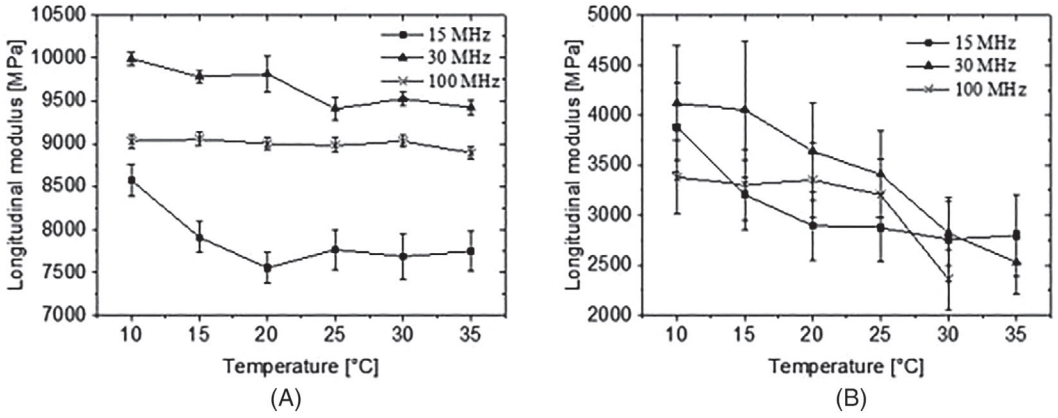

FIGURE 6 Longitudinal modulus of individual BS, A, and EVA, B, foils calculated acoustically. The points correspond to the average of five measurements and the error bars are the error propagation calculation

used to calculate the moduli of BS and EVA nondestructively. The modulus in this case is the longitudinal modulus and is measured through the thickness of the layer.

The values of the longitudinal moduli in both polymeric foils were calculated using Equations (1) and (2) and they are depicted in Figure 6. The measured values for density (Figure 2), thickness (Figure 3) and TOF (Figure 5) at each temperature were used in the calculation.

Similar to the tensile tests (Figure 4), the results show that the longitudinal modulus in both polymeric materials decreases with increasing temperature, as shown in other studies.[15,24,25] In both foils, the modulus is higher at 30 MHz than at 15 MHz. This behavior is in accordance with the time-temperature superposition principle, which states that an increase in frequency and temperature corresponds to opposite effects on the acoustic properties.[15] However, similarly to the TOF results, the longitudinal modulus at 100 MHz for BS tends to remain constant, as depicted in Figure 6A. The longitudinal modulus of the EVA responds more sensitively to temperature than the BS foil. An increase in the TOF corresponds to a decrease in the longitudinal sound speed. This trend has been shown elsewhere at a similar temperature and frequency range.[24]

Moreover, the magnitudes of the Young's modulus are about 50% of the longitudinal modulus in the BS foil and about 0.3% in the EVA foil. Since polymer chain mobility in viscoelastic materials strongly depends on the rate of applied stress, the moduli in these materials depend on the frequency. That is, high frequency measurements are only able to induce motion within very short time scales; hence, high frequency moduli will be considerably higher than low frequency moduli.[15] Presumably, a shift in the T_g is also expected toward measurements at the MHz range following the time-temperature superposition principle since the polymeric materials present much lower chain mobility at high frequencies. Therefore, these materials require higher temperatures in order to increase chain mobility and transition from a glassy to rubbery state.[15,25]

3.4 | Acoustic properties of the BS and EVA foils inside a PV module

The next step is to measure the longitudinal moduli of both polymeric layers laminated in a PV module (glass/EVA/BS). Before, acoustic images of the whole module area were carefully examined for any structural imperfections within the foils and between their interfaces that could affect TOF measurements, such as air gaps, bubbles, impurities, microcracks and other material discontinuities. Since these imperfections reflect the acoustic wave, they give rise to echoes at positions that do not correspond to the foil boundaries, which ultimately masks the real-delay time, that is, the TOF, of the foils and hence their longitudinal modulus (see Figure 1). Likewise, uneven foil thickness, particularly the EVA at the edge of laminated modules and cell gaps[16,18] must be taken into consideration since different thickness also means different TOF for the same material. Assuming the same foil thickness at regions of changing TOF ultimately yields wrong modulus values. Therefore, only defect-free and homogenous areas in the modules were selected for the acoustic measurements.

The TOF in the BS and EVA foils in the PV module as a function of temperature at different frequencies are shown in Figure 7. Although the magnitude of the TOF in the EVA in the module is larger than that in the single foil (Figure 5B),

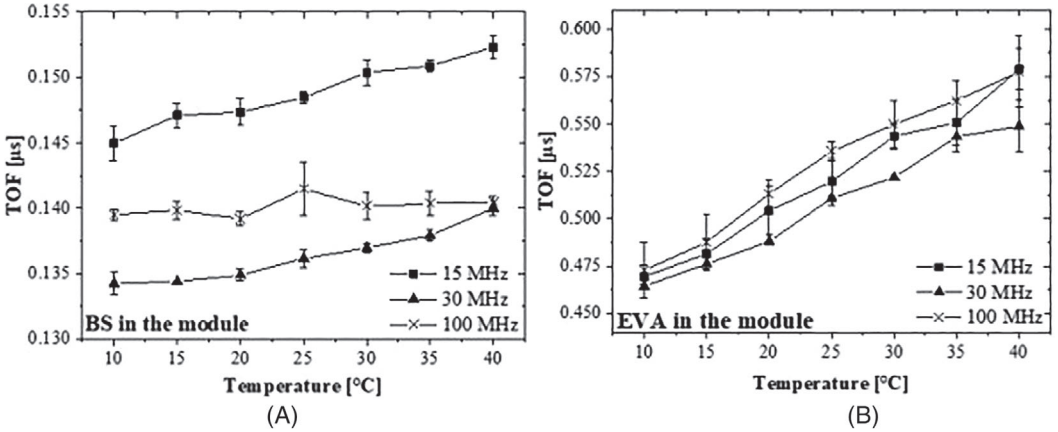

FIGURE 7 Time-of-flight in the BS, A, and EVA, B, in the PV module as a function of temperature. The points correspond to the average of five measurements and the error bars show the respective SDs

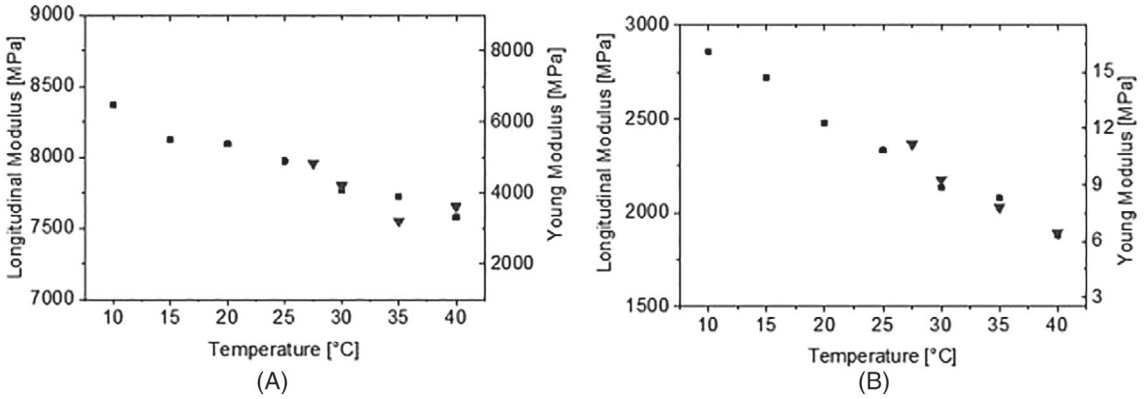

FIGURE 8 Longitudinal modulus (■) and Young Modulus (▼) (values extracted from Figure 4) of BS, A, and EVA, B, foils in the PV module as a function of temperature measured at 15 MHz

the profiles are very similar to those of the freestanding foils presented in Figure 5. In this way, it is validated that the TOF of the BS and EVA can be measured individually, also when they are laminated together. Two reasons might explain the difference in TOF values between foils and modules. The first might result from the variation in mechanical stability of EVA as a freestanding foil and laminated between glass and BS. The second might be related to local variations in the thickness of the EVA foil since this foil melts and fills in gaps between the solar cells during the lamination, which might ultimately lead to uneven thickness across the foil inside the module.[18] Therefore, acknowledging the influence these two factors might have on TOF measurements, this topic remains as the subject of further research.

Similar to the freestanding BS foil in Figure 6A, the TOF trend in the BS in the module also remains constant at 100 MHz. A consideration must be noted about the comparison of low frequency measurements, for example, tensile tests and dynamic mechanical analyses (DMA), with high frequency measurements, for example, ultrasonic methods, considering that the elastic moduli in polymers depend on the frequency. At high ultrasound frequencies, the actual physical deformation incurred in the polymer is very small as a result of the extreme short time of the wave passage. In other words, the stress of the high frequency ultrasound is exerted in the material for a very short time, leaving short-length scales for the relaxation of molecular chains.[15] This may explain the loss of correlation between the BS and the temperature at 100 MHz. In addition, this also explains why the magnitude values of the modulus measured acoustically are much higher than the modulus measured by the tensile test. In order for a polymer to be able to respond to stresses at higher frequency ranges, it must be relatively softer.[25] Therefore, this might explain the difference observed in the acoustic properties between the stiffer BS and the softer EVA foil at 100 MHz. Thus, this high frequency should not be used for the measurement of the moduli of PET-based BSs as used here. The frequency of 15 MHz was chosen for the measurement of longitudinal moduli of the polymeric layers in PV module. The longitudinal moduli of the BS and EVA foils inside the PV module at 15 MHz are depicted in Figure 8. The L values were calculated using the Equations (1) and (2).

Constant foil density (Figure 2) and thickness (Figure 3) along the temperature range studied were assumed. The values of these parameters at 25°C were chosen. For BS the density used is 1462 kg/m^3 and thickness 173 μm, for EVA the density is 949 kg/m^3 and thickness 407 μm. A decreasing trend in the longitudinal modulus with increasing temperature was also observed in the foils inside the module.

In Figure 8 the longitudinal and Young moduli of the individual foils are plotted in order to show the agreement between these two parameters. The changes in elastic moduli in the chosen temperature range follow the same trend. The absolute values differ considerably, which is justified by the different frequency used.

4 | CONCLUSIONS

This study presented the verification of SAM as a nondestructive method for the measurement of the longitudinal modulus of backsheet and EVA foil inside a PV module. On the basis of the approach presented in this study, the estimation of the absolute value of the acoustic properties of the polymeric foils requires, therefore, the measurement of the thickness and density of the foils in the PV module. By considering that these parameters remain constant across a given temperature range, the change in longitudinal modulus can be calculated. First, it was shown that tensile tests and acoustic measurements produced similar trends but different absolute values for the moduli in the selected temperature range, which is assigned to the differences in frequency used during the measurements. It was shown that the longitudinal modulus in the BS and the fast-cure EVA have a similar trend with temperature in both foil configurations (as freestanding foils and laminated as a PV module). Although SAM and tensile tests measure the elastic modulus of the polymeric foils at different directions, the change of the modulus of these materials at 15 MHz has a good correlation with the Young's modulus calculated from the tensile tests. Moreover, the differences in the results between both BS and EVA foils at 100 MHz seem to indicate a critical frequency range at which acoustic measurements should be conducted. At 100 MHz, it was not possible to verify sensitive temperature-dependent changes in the BS. Acoustic measurements at a wider frequency range are needed to understand the resulting behavior of these polymeric materials more precisely. Therefore, SAM measurements at 15 MHz can be used to evaluate viscoelastic changes in polymeric layers in a PV module caused by aging as long as the temperature during the measurement is controlled.

Further research should focus on deriving the thickness and density of these polymeric materials simultaneously to eliminate the need to input variables, which must be determined elsewhere. The next step would be to adapt our system for generating shear waves to determine the shear modulus, and then, enable a full characterization of the mechanical properties of PV module BS and encapsulation foils nondestructively.

ACKNOWLEDGEMENTS

The authors kindly thank Philipp Hügenell and Georg Hagelstein for the density and thickness measurements, respectively. They also thank Tatjana Djuric-Rissner from PVA Tepla, Germany, for the assistance with the acoustic measurements.

PEER REVIEW INFORMATION

Engineering Reports thanks Ebrahim Najafi, Gernot M. Wallner, and other anonymous reviewer(s) for their contribution to the peer review of this work.

CONFLICT OF INTERESTS

All the authors declare that they have no conflict of interest relevant to this article.

AUTHOR CONTRIBUTIONS

Laila V. Mesquita lead conceptualization, data curation, formal analysis, writing—original draft, supported investigation, and contributed equally to the methodology, project administration, software, and validation. **Djamel Eddine Mansour** equally contributed to the conceptualization, visualization, and writing—review and editing. **Paul Gebhartd** supported supervision, writing—original draft. **Luciana Pitta Bauermann** contributed equally to the conceptualization, methodology, and writing—review and editing, lead project administration, supervision, and supported writing-original draft.

ORCID

Luciana Pitta Bauermann https://orcid.org/0000-0001-6333-8525

REFERENCES

1. Omazic A, Oreski G, Halwachs M, et al. Relation between degradation of polymeric components in crystalline silicon PV module and climatic conditions: a literature review. *Solar Energy Mater Solar Cells*. 2019;192:123-133. https://doi.org/10.1016/j.solmat.2018.12.027.
2. King DL, Quintana MA, Kratochvil JA, Ellibee DE, Hansen BR. Photovoltaic module performance and durability following long-term field exposure. *Prog Photovoltaics: Res Appl*. 2000;8(2):241-256. https://doi.org/10.1002/(SICI)1099-159X(200003/04)8:2<3C241::AID-PIP290>3E3.0.CO;2-D.
3. Oreski G, Wallner GM. Aging mechanisms of polymeric films for PV encapsulation. *Solar Energy*. 2005;79(6):612-617. https://doi.org/10.1016/j.solener.2005.02.008.
4. Agroui K, Collins G, Giovanni F, Stark W. A comprehensive indoor and outdoor aging of the cross-linked EVA Encapsulant material for photovoltaic conversion. *Polym Plast Technol Eng*. 2015;54(7):719-729. https://doi.org/10.1080/03602559.2014.974278.
5. Köntges M, Kurtz S, Packard C, Jahn U, Berger K, Kato K, Friesen T, Liu H, Iseghem MV.. Review of Failures of Photovoltaic Modules: Performance and Reliability of Photovoltaic Systems Subtask 3.2: Report IEA-PVPS T13-01:2014. Sankt Ursen, CH; 2014. https://iea-pvps.org/key-topics/review-of-failures-of-photovoltaic-modules-final/
6. Voronko Y, Eder G, Weiss M, et al. Long term performance of PV modules: system optimization through the application of innovative non-destructive characterization methods. *Proceedings of the 27th EU PVSEC*. Frankfurt: 2012:3530-3535. https://doi.org/10.4229/27THEUPVSEC2012-4BV.3.41.
7. Schlothauer JC, Grabmayer K, Wallner GM, Röder B. Correlation of spatially resolved photoluminescence and viscoelastic mechanical properties of encapsulating EVA in differently aged PV modules. *Prog Photovoltaics Res Appl*. 2016;24(6):855-870. https://doi.org/10.1002/pip.2734.
8. Knausz M, Oreski G, Eder GC, et al. Degradation of photovoltaic backsheets: comparison of the aging induced changes on module and component level. *J Appl Polym Sci*. 2015;132(24):42093(1-42093(8. https://doi.org/10.1002/app.42093.
9. Lloyd J, Christian T, Doble D, Mickiewicz RA. (2011). Non-destructive measurement of the degree of cross-linking of eva solar module encapsulation, in Photovoltaic Specialists Conference (PVSC), 37th IEEE, pp. 2273-2278, IEEE; 2011. https://doi.org/10.1109/PVSC.2011.6186408.
10. Lellinger D, Tadjbach S, Alig I. Determination of the elastic moduli of polymer films by a new ultrasonic reflection method. *Macromol Symp*. 2002;184(1):203-214. https://doi.org/10.1002/1521-3900(200208)184:1<203::AID-MASY203>3.0.CO;2–8.
11. Hirschl C, Biebl M, Rydlo M, et al. Determining the degree of crosslinking of ethylene vinyl acetate photovoltaic module encapsulants—a comparative study. *Solar Energy Mater Solar Cells*. 2013;116:203-218. https://doi.org/10.1016/j.solmat.2013.04.022.
12. Carlson JE, Van Deventer J, Scolan A, Carlander C. Frequency and temperature dependence of acoustic properties of polymers used in pulse-Echo Systems. *IEEE Ultrasonics Symposium*. 2003;1:885-888. https://doi.org/10.1109/ULTSYM.2003.1293541.
13. Mühleisen W, Biebl-Rydlo M, Spielberger M. Determining the degree of EVA cross-linking in assembled PV modules acoustically and in-situ. *Proceedings of the 26th EU PVSEC*. Hamburg: 2011:3480-3483. https://doi.org/10.4229/26thEUPVSEC2011-4AV.1.59.
14. Briggs G. Acoustic microscopy-a summary. *Rep Prog Phys*. 1992;55(7):851-909. https://doi.org/10.1088/0034-4885/55/7/001.
15. Sinha M, Buckley DJ. Acoustic properties of polymers. In: Mark JE, ed. *Physical Properties of Polymers Handbook*. New York, NY: Springer; 2007:1021-1031. https://doi.org/10.1007/978-0-387-69002-5_60.
16. Mesquita LV, Mansour DE, Philipp D, Pitta Bauermann L. Scanning acoustic microscopy as a non-destructive method for the investigation of PV module components. *Proceedings of the 35th EU PVSEC*. Brussels: 2018:1318-1322. https://doi.org/10.4229/35thEUPVSEC20182018-5CV.3.23.
17. Mesquita LV, Klasen N, Fokuhl E, Philipp D, Pitta Bauermann L. Analysis of shingle interconnections in solar modules by scanning acoustic microscopy. *AIP Conf Proc*. 2019;2147:090003(1–8). https://doi.org/10.1063/1.5123871.
18. Pfreundt A, Yucebas D, Beinert AJ, et al. Post-processing thickness variation of PV module materials and its impact on temperature, mechanical stress and power. *Proceedings of the 36th EU PVSEC*. Marseille; 2019:935-940. https://doi.org/10.4229/EUPVSEC20192019-4CO.4.3.
19. Seitz JT. The estimation of mechanical properties of polymers from molecular structure. *J Appl Polym Sci*. 1993;49(8):1331-1351. https://doi.org/10.1002/app.1993.070490802.
20. Deutsches Institut für Normung e.V. (DIN) (2003). *DIN EN ISO 527-3 - Kunstoffe Bestimmung der Zugeigenschaften. Teil 3 -Prüfbedingungen für Folien und Tafeln* (DIN EN ISO, DIN EN ISO 527-3). Berlin: Beuth Verlag GmbH.
21. Parker NG, Mather ML, Morgan SP, Povey MJW. Longitudinal acoustic properties of poly(lactic acid) and poly(lactic-co-glycolic acid). *Biomed Mater*. 2010;5(5):55004. https://doi.org/10.1088/1748-6041/5/5/055004.
22. Geretschläger KJ, Wallner GM, Fischer J. Structure and basic propertiesof photovoltaic module backsheet films. *Solar Energy Mater Solar Cells*. 2016;144:451-456. https://doi.org/10.1016/j.solmat.2015.09.060.
23. Li H-Y, Perret-Aebi L-E, Théron R, Ballif C, Luo Y, Lange RFM. Optical transmission as a fast and non-destructive tool for determination of ethylene-co-vinyl acetate curing state in photovoltaic modules. *Prog Photovoltaics Res Appl*. 2013;21(2):187-194. https://doi.org/10.1002/pip.1175.
24. Mott PH, Roland CM, Corsaro RD. Acoustic and dynamic mechanical properties of a polyurethane rubber. *J Acoust Soc Am*. 2002;111(4):1782-1790. https://doi.org/10.1121/1.1459465.

25. McHugh J, Döring J, Stark W, Guey JL. Relationship between the Mechanical and Ultrasound Properties of Polymer Materials. In Proceedings of the 9th European Conference on NDT, Berlin, 11, 1-9, 2006. http://dx.doi.org/10.14279/depositonce-1706.

How to cite this article: Mesquita LV, Mansour DE, Gebhardt P, Pitta Bauermann L. Scanning acoustic microscopy analysis of the mechanical properties of polymeric components in photovoltaic modules. *Engineering Reports*. 2020;e12222. https://doi.org/10.1002/eng2.12222